# UWB FOR NONINVASIVE WIRELESS BODY AREA NETWORKS: CHANNEL MEASUREMENTS AND RESULTS

Thomas Zasowski[1], Frank Althaus[1], Mathias Stäger[2], A. Wittneben[1], and G. Tröster[2]

Swiss Federal Institute of Technology (ETH) Zurich
[1] Communication Technology Laboratory, Sternwartstrasse 7, CH-8092 Zurich
[2] Electronics Laboratory, Gloriastrasse 35, CH-8092 Zurich
Email: {zasowski, althaus, wittneben}@nari.ee.ethz.ch, {staeger, troester}@ife.ee.ethz.ch

***Abstract*— The paper presents UWB channel measurements from 3 to 6 GHz for a body area network (BAN) in an anechoic chamber and an office room. Both, transmit and receive antenna were placed directly on the body. Channel parameters as delay spread and path loss are extracted from the measurements and the influence of the body is highlighted. We show that in some situations there are significant echoes from the body (e.g. from the arms) and we observed deterministic echoes from the floor that could help to simplify a RAKE receiver structure. Finally, we consider the overall energy consumption of the BAN and give decision regions for singlehop and multihop links in relation to signal processing energy.**

## 1. INTRODUCTION

Wireless Body Area Networks (WBANs) are networks whose nodes are usually placed close to the body on or in everyday clothing [1]. A WBAN topology comprises many *transmit only sensor nodes*, that have to be very simple, low cost and extremely energy efficient, some *transceiver nodes*, that afford a somewhat higher complexity to sense and act, and few *high capability nodes*, e.g. master nodes with high computational capabilities and support for higher data rates.

Compared to other wireless networks a WBAN has some distinct features and requirements. Due to the close proximity of the network to the body, electromagnetic pollution should be extremely low. Thus, a noninvasive WBAN requires a low transmit power. Therefore a multihop approach is promising: A sensor does not transmit its data directly to a master node but the data is forwarded by several nodes. Furthermore WBANs have a special network topology since it is given by the shape of the human body. In contrast to indoor channels, the permanent presence of the body could lead to deterministic channel characteristics which could be exploited to simplify the receiver design.

A possible technology for noninvasive WBAN communication is Ultra Wideband (UWB) [2]. In this paper we investigate the UWB WBAN channel. Based on channel measurements from 3 to 6 GHz, we determine channel parameters as delay spread and path loss and illustrate the influence of the body and the environment. We then describe the impact of our results on the design of UWB WBAN systems.

## 2. RELATED WORK

UWB channel measurements for indoor and outdoor communications have been published, e.g. in [3], [4], [5], [6]. But these measurements do not consider the influence of the human body on the channel. The influence of the human body on wideband and ultra wideband channel characteristics was investigated in [7] and [8] but only for one antenna mounted on the body, whereas the second antenna was farther away. To the authors' knowledge, no UWB channel measurements with both antennas placed on the body have been presented yet.

## 3. MEASUREMENT SETUP

UWB WBAN measurements were performed in the frequency range from 3 to 6 GHz. A network analyzer and two meander line antennas (Skycross SMT-3TO6M) were used to measure the S–Parameter $S_{21}$. The measurements were performed in an anechoic chamber and in a small office room with metallic desks and cabinets to compare two extremes. The measurements in the anechoic chamber were made to expose the impact of the body and thus to extract the deterministic part of the BAN channel.

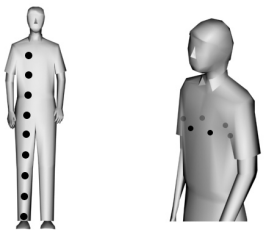

Fig. 1. Antenna placement for measurements on the front side of the body (left) and around the upper torso (right).

In both environments two different series of measurements were made: measurements on the front side of the body and measurements around the upper torso. In all measurements the antennas were directly placed on the body or on the clothes.

Along the front side of the body 9 equidistant points (15cm apart) were defined (see Fig. 1 left). Measurements from each node to each other were performed, which results in 216 single measurements. On the upper

part of the body ($\approx$ 140cm above the floor) 6 points around the torso having similar distances from one to the next were chosen. Two points were defined on the front side of the chest, two on the back and one on each side of the chest (see Fig. 1 right). In total 88 frequency transfer functions were measured around the upper torso.

## 4. Measurement Results

Based on the measured frequency transfer functions, consisting of 1601 frequency points, channel impulse responses are computed by an inverse Fourier transform and evaluated. The results of the two different measurement series are presented separately. In each series, measurements with the same distance are evaluated together.

### *4.1. Measurements on the front side of the body*

*a) Mean delay of strongest echo:* In Fig. 2 the mean delays of the echoes with the highest energy are plotted for different distances between transmit and receive antenna. The curve for the anechoic chamber shows a linear increase of about 0.5ns per 15cm. This corresponds to a dominant direct path between transmit and receive antenna. The curve for the office room shows the same behavior for distances of up to 30cm. For higher distances the direct path is not for all channels the dominant path.

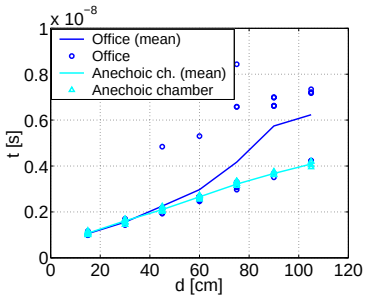


Fig. 2. Mean delay of strongest echo

*b) Mean Excess Delay $\tau_m$ and Delay Spread $\tau_{rms}$:* To characterize the power delay profile we use the mean excess delay $\tau_m$ which is the first central moment of $|h(\tau)|^2$ and the delay spread $\tau_{rms}$ which is the square root of the second central moment of $|h(\tau)|^2$ [9]. The mean excess delay $\tau_m$ is defined as

$$\tau_m = \frac{\int_0^\infty \tau \cdot |h(\tau)|^2 d\tau}{\int_0^\infty |h(\tau)|^2 d\tau} \tag{1}$$

and the delay spread $\tau_{rms}$ as

$$\tau_{rms} = \sqrt{\frac{\int_0^\infty (\tau - \tau_m)^2 \cdot |h(\tau)|^2 d\tau}{\int_0^\infty |h(\tau)|^2 d\tau}} \tag{2}$$

For evaluation of $\tau_m$ and $\tau_{rms}$ we consider a 100ns interval of the channel impulse response since echoes from obstacles fade away after this time. Mean values of $\tau_{rms}$ and $\tau_m$ are shown in Tab. 1. It is obvious that the multipath components caused by the body are small compared to the ones caused by the office environment. For example, at distances of 105cm the delay spread is $\tau_{rms} = 2.2$ns in the anechoic chamber whereas it is $\tau_{rms} = 7.5$ns in the office. The latter is similar to the value given in [10] ($\tau_{rms} = 8.13$ns) for a distance of 1m in a line-of-sight office scenario.

| Distance [cm] | Office | | Anechoic chamber | |
|---|---|---|---|---|
| | $\tau_{rms}$ [ns] | $\tau_m$ [ns] | $\tau_{rms}$ [ns] | $\tau_m$ [ns] |
| 15 | 2.1 | 1.4 | 1.4 | 1.2 |
| 30 | 3.2 | 2.6 | 1.5 | 1.8 |
| 45 | 4.1 | 4.2 | 1.6 | 2.4 |
| 75 | 5.8 | 7.2 | 1.9 | 3.6 |
| 105 | 7.5 | 11.3 | 2.2 | 4.7 |

Tab. 1. Delay spread $\tau_{rms}$ and mean excess delay $\tau_m$ for the measurements on the front side of the body

*c) Path Loss:* The path loss can be calculated directly from the measured frequency transfer functions [5]. If there are $j = 1, \ldots, M$ transfer functions available for a distance $d$ with $i = 1, \ldots, N$ frequency points the path loss is

$$\mathrm{Pl}(d) = \frac{1}{MN} \cdot \sum_{i=1}^{N} \sum_{j=1}^{M} \left| H_j^{(d)}(f_i) \right|^2 \tag{3}$$

$H_j^{(d)}(f_i)$ denotes the $j^{\text{th}}$ frequency transfer function at a frequency $f_i$ in a distance $d$. Since $\mathrm{PL}(d) \propto d^\gamma$ the path loss exponent $\gamma$ can be evaluated at any distance $d$ as described in [9]

$$\mathrm{PL}(d) = \mathrm{PL}_0 + 10 \cdot \gamma \cdot \log_{10}\left(\frac{d}{d_0}\right) \tag{4}$$

with $\mathrm{PL}_0$ as path loss at distance $d_0$. We set $d_0 = 1$m for better comparison with existing results. Therefore, for distances $d < 1$m the second addend in (4) becomes negative. To determine the path loss $\mathrm{PL}(d)$, which includes in this case attenuation, reflection and diffraction effects, we perform a least square fit computation and get

$\mathrm{PL}_0 = 82.0$ dB , $\quad \gamma = 3.3 \quad$ (anechoic chamber)
$\mathrm{PL}_0 = 75.8$ dB , $\quad \gamma = 2.7 \quad$ (office)

Measured and modelled path loss for the anechoic chamber and the office room are shown in Fig. 3. Path loss exponents given in [4], [5], [11] for non line–of–sight measurements in office and in–home environments range from $\gamma = 1.96$ to $\gamma = 3.5$. Our evaluated path losses are located in the upper region of this range. In the case of the anechoic chamber measurements ($\gamma = 3.29$) the high value is a direct consequence of the non-reflecting environment. As expected, the path loss in the office environment is lower ($\gamma = 2.67$), but we can still anticipate a relatively high value since the human body attenuates the echoes coming from the back side.

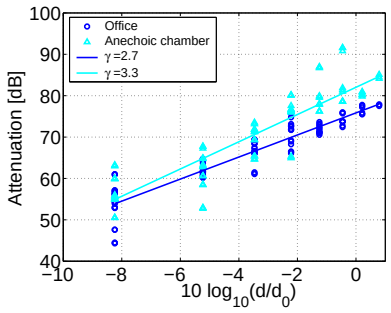


Fig. 3. Path loss along the front side of the body for anechoic chamber and office measurements

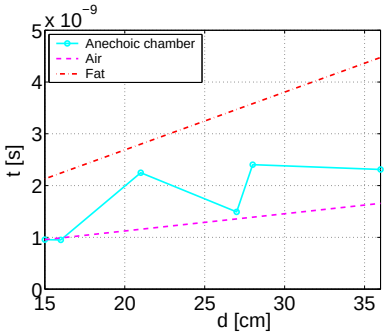


Fig. 4. Mean delay of strongest echo in anechoic chamber for measurements around the upper part of the body

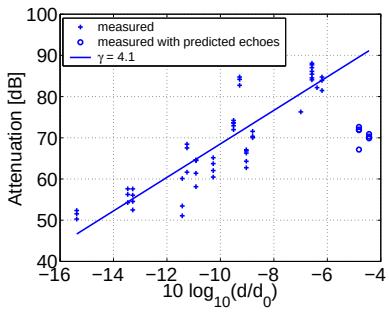


Fig. 5. Path loss for links through the human body

### *4.2. Measurements around the torso*

Although distances between nodes on the torso are relatively small, we expect a stronger attenuation of the transfer function caused by the body. Position and distances for nodes placed on the torso are illustrated in Fig. 7(a). In our case we encounter distances of 15cm, 16cm, 21cm, 27cm, 28cm and 36cm.

*a) Mean delay of strongest echo:* For measurements where both antennas are placed on the same side of the body, the direct path is the dominant path and the number of echoes is similar to the ones discussed in section 4.1. If the antennas are placed on opposite sides of the body, the direct path is attenuated severely and an significant echo by the floor can be observed in the office environment. This deterministic echo could be exploited by a simple RAKE receiver.

Fig. 4 shows the mean delay of the echoes with the highest energy for the anechoic chamber. It is obvious from Fig. 7(a) that for the 15cm/16cm link the direct path is a quasi line-of-sight path. For larger distances, i.e. antennas placed on opposite sides of the body, the delays are much higher than the expected delays for a line-of-sight channel. This effect can be explained by taking into account the different propagation velocities for different tissues given in [12] and the echoes off the body itself.

*b) Path Loss:* Since some of the measurements are determined by the medium air and others by the body, a path loss cannot be given explicitly. To calculate a path loss which is mainly dominated by the body itself, we performed further measurements. Therefore, we placed both antennas on opposite sides of arms, legs and the upper part of the body. Evaluating these measurements we get

$$\mathrm{PL}_0 = 109.2 \text{ dB} , \quad \gamma = 4.1$$

using a least square fit. The measured values and $\mathrm{PL}(d)$ are displayed in Fig. 5. Note that the attenuation and the path loss coefficient $\gamma = 4.1$ for transmission through the human body are higher than for transmissions on the front side of the body. This value can be interpreted as a worst case path loss for the WBAN channel.

An interesting effect can be observed for links where at least one antenna is placed close to an arm. In our case this applies to the 27cm and the 36cm link (see $d = 27$cm and $d = 36$cm in Fig. 4). The mean delay of the strongest echo and the attenuation of these links are lower than expected. This effect is caused due to echoes off the arms. Depending on the position of the arms, variations of up to 20dB in attenuation could be observed. Therefore we ignored those measurements (see circles in Fig. 5) when calculating the path loss through the body. We could not observe those echoes for the other links but expect them to be present, although significantly lower.

*c) Mean Excess Delay $\tau_m$ and Delay Spread $\tau_{rms}$:* For quasi line-of-sight links, the values for the mean excess delay $\tau_m$ and the delay spread $\tau_{rms}$ are similar to the ones presented in Tab. 1. For longer link distances, it can be observed that the values for $\tau_m$ and $\tau_{rms}$ (Tab. 2) are not only dependent on the distance but also on the transmission medium. The higher values for the office measurements can be traced back to the echoes present in this environment.

| Distance [cm] | Office | | Anechoic chamber | |
|---|---|---|---|---|
| | $\tau_{rms}$ [ns] | $\tau_m$ [ns] | $\tau_{rms}$ [ns] | $\tau_m$ [ns] |
| 15 | 2.1 | 1.3 | 1.4 | 1.1 |
| 28 | 9.9 | 18.1 | 7.3 | 5.5 |

Tab. 2. Delay spread and mean excess delay for the torso measurements

## 5. Impact on the Design of WBAN's

### *5.1. Number of RAKE fingers*

One of the most cited receiver structure for UWB signals is the RAKE receiver. It collects the energy in the multipath components of the channel. The complexity

of this receiver increases with the number of its fingers which correspond the number of multipath components that can be collected. Therefore, the distribution of the energy components in the channel impulse responses is of particular interest. In Fig. 6 the cumulative energy of the $L$ strongest paths is displayed for different distances between transmit and receive antenna in the office room. If we demand the RAKE receiver to collect $75\%$ of the whole energy, we need 2 RAKE fingers to transmit over a distance of 15cm. With increasing distance the number of fingers grows up to 20 for 90cm links. To receive the same percentage of energy in the case of the 28cm non line-of-sight link through the body, we would need far more than 20 RAKE fingers.

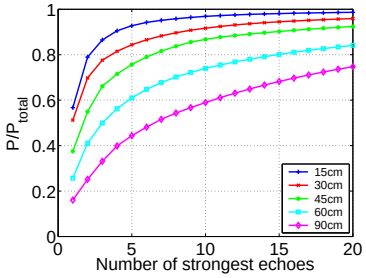


Fig. 6. Cumulative normalized power of the $L$ paths with the highest power in the office room

### *5.2. Energy considerations for single- and multihop links*

Beside relative energies, absolute received energies determine the most appropriate receiver structure and network topology. For a noninvasive wireless BAN the electromagnetic exposure of the human body must be extremely low. Consequently, the radiated energy of one pulse should be limited to a maximum value $E_{rp}$, given a specified pulse shape. To establish network connectivity with such low power constraints, one needs to accumulate several pulses at the receiver for each bit. The number of pulses can be reduced by reducing the distance between two hops. At the same time the number of hops have to be increased. The drawback of this multihop approach is the energy which is dissipated for the signal processing in the relaying nodes. The overall energy is the most important factor determining the lifetime of the network. In this section we study some basic energy relations based on the measurements we made.

The total energy capture per bit, $E_{g,1}$, for a singlehop link using $M_P$ pulses is composed of the energy dissipated for the wave radiation $M_P \cdot E_{rp}$ and the signal processing energy, which is further divided into a part $E_{cp}$ that comprises generating and receiving of a pulse and a part $E_{cb}$ that comprises encoding and decoding of single bits.

$$E_{g,1} = M_P \cdot E_{cp} + E_{cb} + M_P \cdot E_{rp} \tag{5}$$

To determine the minimum number of pulses $M_P$ we assume that a certain SNR per bit of

$$\rho_b = \frac{E_b}{N_0} \tag{6}$$

at the receiver is required to establish a reliable point-to-point link. $N_0 = k \cdot T_{sys}$ is the noise power spectral density and $E_b$ the required energy per bit at the receiver.

Given the gain $G_h$ of the radio channel as the ratio of received energy to transmitted energy, the required radiated energy at the transmitter is

$$E_r = M_P \cdot E_{rp} = \frac{E_b}{G_h} \tag{7}$$

The gain $G_h$ depends on the channel impulse response and on the receiver structure. As in [13] we make two assumptions: a) the receiver has a matched front-end structure and b) the multipath channel is separable. We consider a selective RAKE receiver (SRAKE), which uses the $L$ strongest paths for decoding. Then, the channel gain can be determined from the coefficients $a_i$ of the measured impulse response $h(k) = \sum_{i=1}^{N_r} a_i \delta(k-i)$:

$$G_h = \sum_{i=1}^{L} |a_{(i)}|^2, \tag{8}$$

where $a_{(i)}$ is ordered in a way that $|a_{(1)}| > |a_{(2)}| > \ldots > |a_{(L)}|$, $1 \le L \le N_r$. With equation (6), (7) and (8) the minimum number of pulses $M_P$ (rounded up to the next integer) can be determined as

$$M_P = \left\lceil \frac{\rho_b \cdot N_0}{E_{rp} \cdot \sum_{i=1}^{L} |a_{(i)}|^2} \right\rceil \tag{9}$$

The total energy which is used for a multihop connection with $M_H$ hops is composed of the energies of the $M_H$ single hops:

$$E_{g,M} = \sum_{j=1}^{M_H} \left( M_P^{(j)} \cdot E_{cp} + E_{cb} + M_P^{(j)} \cdot E_{rp} \right), \tag{10}$$

where $M_P^{(j)}$ is number of pulses for the $j$th hop.

In the following we compare the energies for a transmission from one point on the back to one point on the chest. We consider the direct transmission (which means that the body causes a very high attenuation), a double hop link and a triple hop link (see Fig 7(b)). We assume a one finger SRAKE receiver ($L = 1$), $\rho_b = 10$dB and $N_0 = k \cdot T_{sys} \cdot \mathrm{NF} = 4.14 \cdot 10^{-20}$ which corresponds to a temperature $T_{sys}$ of 300K and a noise figure $\mathrm{NF} = 10$. $E_{rp}$ is set to $2 \cdot 10^{-14}$J, which is the energy of a 100ps pulse, respecting the

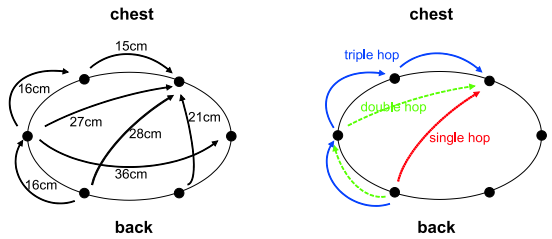


(a) Direct paths (b) Evaluated hops

Fig. 7. Position, distances and multihop paths for nodes around the upper part of body

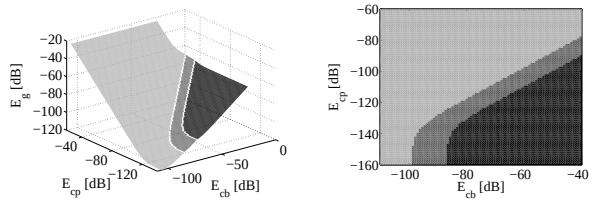


(a) $E_g$ over $E_{cp}$ and $E_{cb}$ (b) 2D-Projection of (a)

Fig. 8. Energy comparison: minimum total energy per bit $E_g$ is achieved with: 1 hop (black), 2 hops (gray), 3 hops (light)

FCC UWB mask in the band from 3 to 6 GHz. Fig. 8 illustrates the regions where the different transmission strategies are to prefer. In Fig. 8(a) the minimum total energy per bit, $\min(E_{g,1}, E_{g,2}, E_{g,3})$, for all values of $(E_{cp}, E_{cb})$ is plotted over the signal processing energies $E_{cp}$ and $E_{cb}$. The different shades of gray indicate where the different transmission strategies contribute to the minimum. Fig. 8(b) shows a 2D-projection into the $E_{cp}$-$E_{cb}$ plane to allow better reading of the values. The energies are given in dB normalized to 1 J. It can be seen that for $E_{cb} < 1$nJ multihop connections are generally to prefer. For $E_{cb} \gg 1$nJ the region for using multihops is given by $E_{cp} > E_{cb} - 40$dB. This means for $E_{cp} > E_{cb} \cdot 10^{-4}$ a multihop strategy should be used for the WBAN.

## 6. Conclusions

Body area network channel measurements were performed from 3 to 6 GHz in an anechoic chamber and an office room. The channels on the front side of the body show line-of-sight properties apart from the path loss which shows non line-of-sight characteristics due to the body's attenuation. The channels around the torso are strongly dependent on the transmission medium. For channels through the human body a path loss exponent of $\gamma = 4.1$ could be evaluated. Thereby, it was observed that echoes off both arms can change the attenuation from the left to the right side of the body by up to 20dB depending on the position of the arms. Moreover, a deterministic echo caused by the floor was observed which could be exploited by a simple RAKE receiver. We have also shown that a RAKE receiver with only 1 or 2 fingers is sufficient to collect 50% or 80% of the maximum energy for links with a distance of 15cm, independently on its placement on the body. An energy comparison for a transmission from a node on the back to a node on the chest has shown that a multihop strategy is recommended if the energy for pulse generation and reception is higher than a ten thousandth part of the energy for bit encoding and decoding.

## References


[1] J. Bernhard, P. Nagel, J. Hupp, W. Strauss, and T. von der Grün, "BAN - Body area network for wearable computing," in *9th WWRF Meeting, Zurich*, July 2003.

[2] D. Porcino and W. Hirt, "Ultra-wideband radio technology: Potential and challenges ahead," in *IEEE Communications Magazine, Vol. 41, No. 7*, July 2003, pp. 66–74.

[3] D. Cassioli, M. Z. Win, and A. F. Molisch, "A statistical model for the UWB indoor channel," in *IEEE 53rd Vehicular Technology Conference, VTC 2001 Spring, Vol. 2*, May 2001, pp. 1159–1163.

[4] J. Kunisch and J. Pamp, "Measurement results and modeling aspects for the UWB radio channel," in *IEEE Conference on Ultra Wideband Systems and Technologies, UWBST*, 2002, pp. 19–23.

[5] S. S. Ghassemzadeh, R. Jana, C. W. Rice, W. Turin, and V. Tarokh, "A statistical path loss model for in-home UWB channels," in *IEEE Conference on Ultra Wideband Systems and Technologies, UWBST*, 2002, pp. 59–64.

[6] R. J.-M. Cramer, R. A. Scholtz, and M. Z. Win, "Evaluation of an ultra-wide-band propagation channel," in *IEEE Transactions on Antennas and Propagation, Vol. 50, No.5*, May 2002, pp. 561–569.

[7] M. Sanchez, L. de Haro, A. Pino, and M. Calvo, "Human operator effect on wide-band radio channel characteristics," in *IEEE Transactions on Antennas and Propagation, Vol.: 45 Issue: 8*, August 1997, pp. 1318–1320.

[8] T. B. Welch, R. L. Musselman, B. A. Emessiene, P. D. Gift, D. K. Choudhury, D. N. Cassadine, and S. M. Yano, "The effects of the human body on UWB signal propagation in an indoor environment," in *IEEE Journal on Selected Areas in Communications, Vol. 20, No. 9*, December 2002, pp. 1778–1782.

[9] J. D. Parsons, *The Mobile Radio Propagation Channel*, 2nd ed. John Wiley & Sons LTD, 2000.

[10] J. Keignart and N. Daniele, "Channel sounding and modelling for indoor UWB communications," in *International Workshop on Ultra Wideband Systems, IWUWBS*, June 2003.

[11] P. Pagani, P. Pajusco, and S. Voinot, "A study of the ultra-wide band indoor channel: Propagation experiment and measurement results," in *International Workshop on Ultra Wideband Systems, IWUWBS*, June 2003.

[12] E. M. Staderini, "UWB radars in medicine," in *IEEE AESS (Aerospace & Electronic Systems Society) Systems Magazine*, January 2002, pp. 13–18.

[13] M. Z. Win and R. Scholtz, "On the energy capture of ultrawide bandwidth signals in dense multipath environments," in *IEEE Communications Letters, Vol. 2*, September 1998, pp. 245–247.